

**Origin of magnetic inhomogeneity in Cr- and V-doped topological insulators**Shifei Qi,<sup>1,2,\*</sup> Zheng Liu,<sup>2,\*</sup> Maozhi Chang,<sup>3,1</sup> Ruiling Gao,<sup>3,1</sup> Yulei Han,<sup>2,†</sup> and Zhenhua Qiao<sup>2,†</sup><sup>1</sup>College of Physics, Hebei Normal University, Shijiazhuang, Hebei 050024, China<sup>2</sup>ICQD, Hefei National Laboratory for Physical Sciences at Microscale, CAS Key Laboratory of Strongly-Coupled Quantum Matter Physics, and Department of Physics, University of Science and Technology of China, Hefei, Anhui 230026, China<sup>3</sup>Institute of Materials Science, Shanxi Normal University, Linfen, Shanxi 041004, China

(Received 4 February 2020; revised manuscript received 1 May 2020; accepted 8 May 2020; published 1 June 2020)

The quantum anomalous Hall effect (QAHE) has been experimentally observed in magnetically doped topological insulators at ultralow temperatures. Inhomogeneous ferromagnetism is considered to be one of the main factors that lead to the unexpected low QAHE observation temperature. Dopant-induced disorder is usually the origin of the inhomogeneous ferromagnetism. Here, our systematic first-principles calculations demonstrate that inhomogeneous mixing of Bi and Sb in a  $(\text{Bi, Sb})_2\text{Te}_3$  system is the intrinsic origin of inhomogeneous ferromagnetism. Different from diluted magnetic semiconductors, the mixing energy of Cr and V in  $\text{Bi}_2\text{Se}_3$ ,  $\text{Sb}_2\text{Te}_3$ , and  $(\text{Bi, Sb})_2\text{Te}_3$  topological insulators clearly show that magnetic dopants are homogeneously distributed even in the presence of naturally formed crystalline defects. Surprisingly, our study shows that the mixing energies of Sb and Bi in a  $(\text{Bi, Sb})_2\text{Te}_3$  system are all positive in the whole range of doping concentration, indicating that Bi elements in a  $(\text{Bi, Sb})_2\text{Te}_3$  system are inhomogeneously distributed. Moreover, the formation energies of Cr and V suggest that they are relatively easy to substitute Bi sites in Bi inhomogeneously distributed  $(\text{Bi, Sb})_2\text{Te}_3$  systems, which leads to inhomogeneous ferromagnetism of the experimental QAHE system. The influence of the inhomogeneous distribution of Bi on the electronic structures of bulk  $(\text{Bi, Sb})_2\text{Te}_3$  systems is also analyzed. We believe that our finding of the intrinsic origin of magnetic inhomogeneity should be beneficial for the experimental enhancement of the QAHE observation temperature in magnetically doped topological insulators.

DOI: [10.1103/PhysRevB.101.241407](https://doi.org/10.1103/PhysRevB.101.241407)

**Introduction.** The quantum anomalous Hall effect (QAHE) [1–3] is the quantized version of the anomalous Hall effect [4] and exhibits the same electronic transport properties as that of the quantum Hall effect [5], i.e., quantized Hall conductance and vanishing longitudinal resistance. This makes it appealing to design QAHE-based electronic devices due to their dissipationless chiral edge modes. To realize QAHE in  $\mathbb{Z}_2$  topological insulators (TIs), two ingredients are usually required, i.e., spin-orbit coupling and long-range ferromagnetism. After the experimental realization of monolayer graphene [6], more efforts were made to explore the QAHE [7–18]. Among these materials, the presence of linear Dirac dispersion made both graphene and  $\mathbb{Z}_2$  TIs the most hopeful candidates to engineer topologically nontrivial band gaps that exhibit QAHE. Superior to graphene, only ferromagnetism is required in TIs to realize QAHE [19,20]. Besides the magnetic proximity effect [21,22], magnetic-element doping is a more effective approach to induce a magnetic interaction with the surface states of TIs [23–25], as successfully adopted in diluted magnetic semiconductors (DMSs) [26].

Indeed, based on magnetic doping strategies, the QAHE was first observed in Cr- and V-doped  $(\text{Bi, Sb})_2\text{Te}_3$  thin films

[27–30]. However, the extremely low temperature (typically around tens of mK) is still a great challenge for practical applications. Such an unexpected ultralow temperature is usually attributed to the magnetic inhomogeneity [31–34] or the appearance of dissipative conduction channels induced by metallization of the bulklike region in magnetically doped TIs [35]. Empirically, codoping is an effective way to improve the inhomogeneous ferromagnetic order. For example, the QAHE observation temperature was proposed to be highly improved by codoping  $\text{Sb}_2\text{Te}_3$  with *p*-type vanadium and *n*-type iodine dopants [36]. In a follow-up experiment, the observation temperature was indeed enhanced in Cr- and V-codoped  $(\text{Bi, Sb})_2\text{Te}_3$  thin films. At an optimal Cr/V ratio, the QAHE temperature can reach up to 300 mK, an order of magnitude higher than that for single doping, and the Hall hysteresis loop is more squarelike, indicating a reduced magnetic inhomogeneity in Cr- and V-codoped  $(\text{Bi, Sb})_2\text{Te}_3$  thin films [37]. Although inhomogeneous ferromagnetism can be improved by using the codoping method in both magnetically doped TIs [37] and DMSs [38,39], it is still unclear whether the origin of magnetic inhomogeneity in magnetically doped TIs is the same as that in DMSs (both theoretical and experimental studies have confirmed that the phase separation always exists due to a strong attractive interaction between the magnetic dopants [39]).

In this Rapid Communication, we present a systematic investigation of the physical origin of magnetic

\*These authors contributed equally to this work.

†Corresponding authors: hanyulei@ustc.edu.cn; qiao@ustc.edu.cn

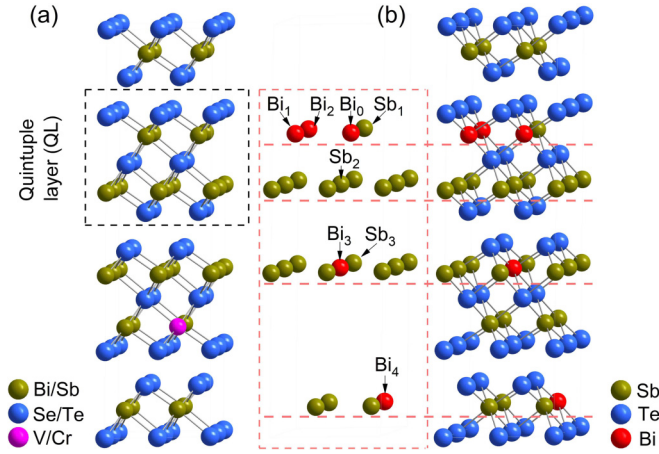


FIG. 1. (a) A  $2 \times 2 \times 1$  supercell of  $\text{Bi}_2\text{Se}_3$  or  $\text{Sb}_2\text{Te}_3$ . (b) A  $2 \times 2 \times 1$  supercell of bulk  $(\text{Bi}, \text{Sb})_2\text{Te}_3$ . To model the inhomogeneously distributed Bi and Sb atoms in a  $(\text{Bi}, \text{Sb})_2\text{Te}_3$  system,  $\text{Bi}_0/1/2$  sites are simultaneously substituted by three Bi atoms in the host  $\text{Sb}_2\text{Te}_3$  system. To model the homogeneously distributed Bi and Sb atoms in a  $(\text{Bi}, \text{Sb})_2\text{Te}_3$  system,  $\text{Bi}_0/3/4$  sites are simultaneously substituted. When calculating the Cr or V formation energy, the substituted sites of Cr or V include  $\text{Bi}_1$ ,  $\text{Sb}_1$ ,  $\text{Sb}_2$ , and  $\text{Sb}_3$ .

inhomogeneity in magnetically doped TIs, by taking examples of three representative host materials, i.e.,  $\text{Bi}_2\text{Se}_3$ ,  $\text{Sb}_2\text{Te}_3$ , and  $(\text{Bi}, \text{Sb})_2\text{Te}_3$ . It is found that the magnetic inhomogeneity originates from the inhomogeneous mixing of Bi and Sb elements in a  $(\text{Bi}, \text{Sb})_2\text{Te}_3$  system, rather than magnetic-atom-induced disorder. This is completely different from the origin of magnetic inhomogeneity in DMSs. Moreover, the formation energies of Cr- and V-doped elements suggest that it is much easier to substitute Bi sites in Bi and Sb inhomogeneously mixed  $(\text{Bi}, \text{Sb})_2\text{Te}_3$ . These findings together reveal the origin of the magnetic inhomogeneity in Cr- and V-doped  $(\text{Bi}, \text{Sb})_2\text{Te}_3$ , and shed light on increasing the QAHE observation temperature in magnetically doped TIs.

**Methods and systems.** Our first-principles calculations were performed by using the projected augmented-wave method [40] implemented in the Vienna *ab initio* simulation package (VASP) [41]. The generalized gradient approximation (GGA) of Perdew-Burke-Ernzerhof type was used to treat the exchange-correlation interaction [42]. For the bulk system, a  $2 \times 2 \times 1$  supercell of a topological insulator is adopted to calculate the mixing energies and bulk band structures [see Fig. 1(a)]. A  $\Gamma$ -centered  $3 \times 3 \times 1$   $k$  mesh was adopted for the structural optimization and the mixing energy calculation, while a  $7 \times 7 \times 2$   $k$  mesh was used for the total energy and band structure calculations. The kinetic energy cutoff was set to be 400 eV. For thin-film calculations, seven quintuple layers, including 56 Se/Sb atoms and 84 Se/Te atoms, were used. A vacuum space of 30 Å was used to avoid spurious interactions. Here,  $k$ -mesh points of  $3 \times 3 \times 1$  and  $7 \times 7 \times 1$  were used for the structure relation and total energy estimation, respectively. The kinetic energy cutoff was set to be 350 eV for the thin-film calculation. All atoms were allowed to relax until the Hellmann-Feynman force on each atom was less than 0.01 eV/Å, and spin-orbit coupling is considered in all calculations. The GGA+ $U$  method [43] was used to treat

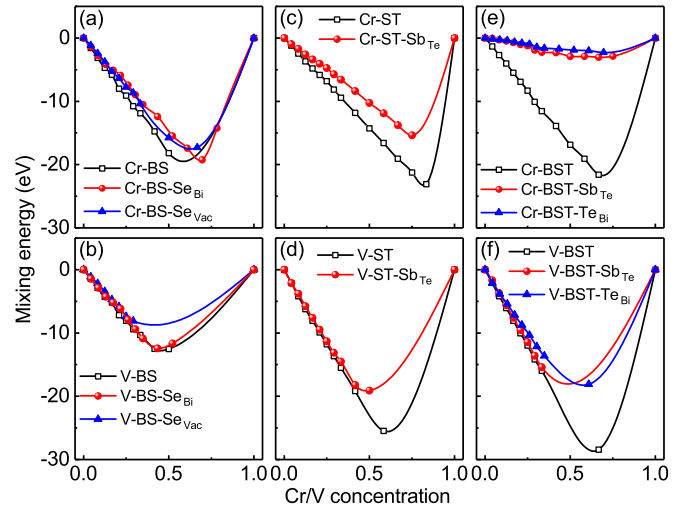


FIG. 2. Mixing energies as a function of doping concentration for Cr- and V-doped (a), (b)  $\text{Bi}_2\text{Se}_3$ , (c), (d)  $\text{Sb}_2\text{Te}_3$ , and (e), (f)  $(\text{Bi}, \text{Sb})_2\text{Te}_3$ . Here, Cr and V atoms are used to substitute the Bi and Sb sites. Systems with intrinsic defects are displayed in red and blue lines, e.g., Cr-BS- $\text{Se}_{\text{Bi}}$  denotes the antisite defect with a Bi site being substituted by a Se atom, whereas Cr-BS- $\text{Se}_{\text{vac}}$  denotes a vacancy at the Se site.

the Coulomb interaction of  $3d$  transition metals, i.e., Cr and V, with  $U = 3.0$  eV and  $J = 0.87$  eV.

The distribution behavior of magnetic atoms in TIs can be estimated from the mixing energy of magnetic atoms, which has been successfully adopted to study the inhomogeneity of DMSs [44,45]. The mixing energy of a two-component material  $A_{1-x}B_x$  can be written as

$$\Delta E = E_{\text{tot}}(A_{1-x}B_x) - (1-x)E_{\text{tot}}(A) - xE_{\text{tot}}(B),$$

where  $E_{\text{tot}}(A_{1-x}B_x)$ ,  $E_{\text{tot}}(A)$ ,  $E_{\text{tot}}(B)$  are respectively the total energies of homogeneously doped, undoped, and completely doped systems, with  $x$  representing the doping concentration.  $\Delta E > 0$  indicates that the system prefers to be in an inhomogeneous state, while  $\Delta E < 0$  indicates a homogeneous state. As displayed in Fig. S1 (see Supplemental Material [46]), we have confirmed the calculation method by repeating a previous finding of a Mn-doped GaAs DMS system [44].

As shown in Fig. 1(b), we choose  $\text{Bi}_1$ ,  $\text{Sb}_1$ ,  $\text{Sb}_2$ , and  $\text{Sb}_3$  as the doping sites of V/Cr atoms. The formation energy of V/Cr substitution at the Bi/Sb site in  $(\text{Bi}, \text{Sb})_2\text{Te}_3$  can be evaluated by using the following expression [47],

$$\Delta E_{\text{F}}(\text{V/Cr}) = E_{\text{tot}}(\text{V/Cr}) - E_{\text{tot}}((\text{Bi}, \text{Sb})_2\text{Te}_3) - \sum_i n_i \mu_i,$$

where  $E_{\text{tot}}(\text{V/Cr})$  and  $E_{\text{tot}}((\text{Bi}, \text{Sb})_2\text{Te}_3)$  denote the total energies of V- and Cr-doped TIs, and  $(\text{Bi}, \text{Sb})_2\text{Te}_3$ , respectively.  $n_i$  is the number of atoms added or removed from  $(\text{Bi}, \text{Sb})_2\text{Te}_3$ . For V/Cr,  $n_i > 0$ , while for Bi/Sb,  $n_i < 0$ .  $\mu$  is the chemical potential of element.

**Homogeneous distribution of magnetic dopants.** We first explore the distribution characteristics of Cr and V dopants in  $\text{Bi}_2\text{Se}_3$ ,  $\text{Sb}_2\text{Te}_3$ , and  $(\text{Bi}, \text{Sb})_2\text{Te}_3$  by calculating the mixing energy  $\Delta E$ . From Fig. 2, one can find that, for all systems, as the doping concentration increases from 0.0 to 1.0, the mixing

energy first decreases from 0.0 to the minimum, then increases to 0.0, showing a concave curve. Moreover, the negative  $\Delta E$  in the whole range of doping concentration indicates that the Cr and V dopants favor the homogeneous distribution. When further considering the intrinsic vacancy or antisite defect, e.g.,  $\text{Se}_{\text{Bi}}$  denotes the antisite defect with a Bi site being substituted by a Se atom, whereas  $\text{Se}_{\text{vac}}$  represents a vacancy at Se site, as displayed in Figs. 2 and S2, one can find that the variation of mixing energy is similar to that of the pristine materials, indicating that the intrinsic defects have a negligible influence on the behavior of the homogeneous dopant distribution. Note that in a Cr-doped  $(\text{Bi}, \text{Sb})_2\text{Te}_3$  system [see Fig. 2(e)], the mixing energies with intrinsic antisite defects are much higher than that of pristine system but still negative, whereas those in a V-doped  $(\text{Bi}, \text{Sb})_2\text{Te}_3$  system are slightly higher than that of pristine material [see Fig. 2(f)], implying that the V element is easier to realize homogeneous doping in  $(\text{Bi}, \text{Sb})_2\text{Te}_3$  with intrinsic defects, which is in agreement with the experimental finding [30].

Thus, our above results confirm that, different from the diluted magnetic semiconductors, the Cr and V dopants in  $\text{Bi}_2\text{Te}_3$ ,  $\text{Sb}_2\text{Te}_3$ , and  $(\text{Bi}, \text{Sb})_2\text{Te}_3$  topological insulators exhibit a homogeneous distribution feature, even in the presence of crystalline defects. As found in the study of DMS that the difference in mixing energies between magnetically doped GaN and GaAs is related to their different band gaps [45,48,49], the qualitative difference of the dopant distribution between TIs and DMSs can be attributed to the large difference between band gaps of the two systems, i.e., the band gaps of the aforementioned three TIs are generally about 0.2–0.3 eV, whereas those of typical DMS (e.g., GaAs or GaN) are about 1.5–3.5 eV.

*The origin of magnetic inhomogeneity.* The experimental observation of magnetic inhomogeneity in doped  $(\text{Bi}, \text{Sb})_2\text{Te}_3$  is usually attributed to magnetic dopants [31–34]. However, our calculations of Cr- and V-doped  $(\text{Bi}, \text{Sb})_2\text{Te}_3$  clearly show that the dopants favor a homogeneous distribution, even in the presence of crystalline defects. To unveil the contradiction, one has to focus on the host  $(\text{Bi}, \text{Sb})_2\text{Te}_3$  system. In experiments, to realize bulk insulating TIs, the mixing strategy of  $\text{Bi}_2\text{Te}_3$  and  $\text{Sb}_2\text{Te}_3$  is adopted due to their opposite charge defects. In reality, the alloying of Bi and Sb should definitely exist in  $(\text{Bi}, \text{Sb})_2\text{Te}_3$ . But the distribution behavior of Bi and Sb in experiment is still unclear. Below, we focused on the mixing energy of Bi in  $\text{Sb}_2\text{Te}_3$ .

As displayed in the Fig. 3(a), the mixing energies of Bi in  $\text{Sb}_2\text{Te}_3$  are provided and the effects of Cr and V doping on the mixing energy are also considered. To our surprise, the mixing energies of Bi in  $\text{Sb}_2\text{Te}_3$  are always positive in the whole range of concentration and exhibit a convex concentration dependence. This is completely opposite to those in Cr- or V-doped TI systems, but similar to those in DMSs. Furthermore, the additional Cr or V doping cannot obviously affect the Bi distribution in  $\text{Sb}_2\text{Te}_3$ . In addition, we calculated the bulk and film band structures of homogeneous and inhomogeneous  $(\text{Bi}, \text{Sb})_2\text{Te}_3$  systems, and found a negligible difference between the two systems, indicating that the inhomogeneous distribution of Bi in  $(\text{Bi}, \text{Sb})_2\text{Te}_3$  cannot be well identified by the angle-resolved photoemission spectroscopy measurement.

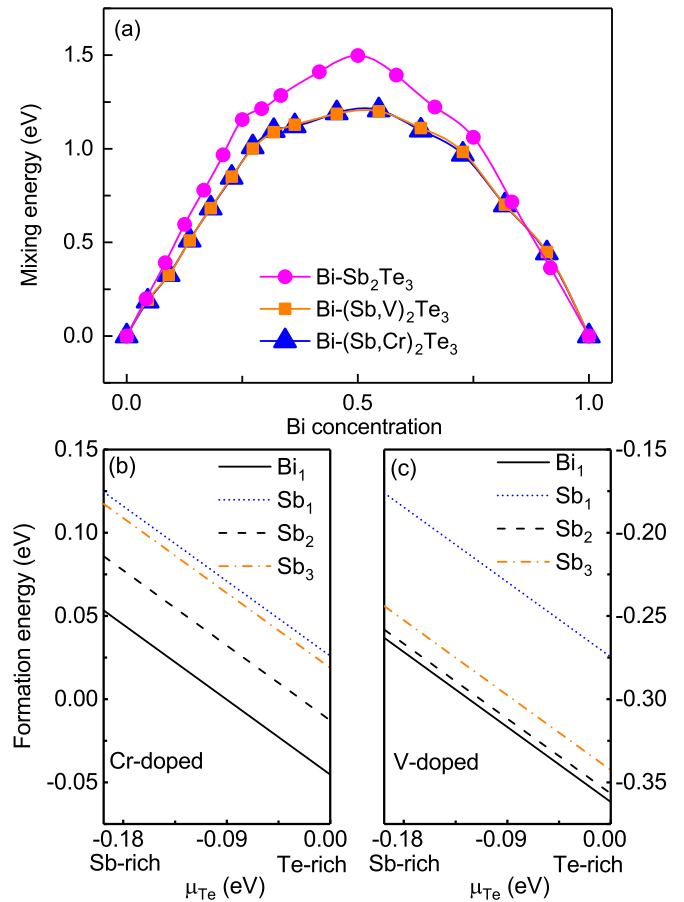


FIG. 3. (a) Mixing energy as a function of dopant concentration for Bi-doped  $\text{Sb}_2\text{Te}_3$ . The influence of V/Cr on mixing energy is also considered as displayed in the orange/blue line. (b) and (c) Formation energies of Cr and V in inhomogeneous  $(\text{Bi}, \text{Sb})_2\text{Te}_3$ . The substituted sites of Cr and V contain  $\text{Bi}_1$ ,  $\text{Sb}_1$ ,  $\text{Sb}_2$ , and  $\text{Sb}_3$ .

Our results confirm that the mixing of Bi and Sb is inhomogeneous in  $(\text{Bi}, \text{Sb})_2\text{Te}_3$  systems. It is noteworthy that, for another three-dimensional (3D) TI  $(\text{Bi}_{1-x}\text{Sb}_x)$  alloy, macroscopic inhomogeneities have been observed in a related experiment [50]. A more related experimental observation of inhomogeneity is from the optoelectronic characterization of  $(\text{Bi}, \text{Sb})_2\text{Te}_3$  [51]. They reported that more inhomogeneous transport properties can be obtained in  $(\text{Bi}, \text{Sb})_2\text{Te}_3$  than in  $\text{Bi}_2\text{Te}_3$ . This in turn proves the possible existence of inhomogeneous mixing of Bi and Sb in  $(\text{Bi}, \text{Sb})_2\text{Te}_3$ .

Let us now move to the substitution behavior of Cr or V dopants in such an inhomogeneous  $(\text{Bi}, \text{Sb})_2\text{Te}_3$  host material. As displayed in Fig. 1(b), to represent the inhomogeneous mixing,  $\text{Bi}_{0,1,2}$  sites are simultaneously substituted by three Bi atoms in  $\text{Sb}_2\text{Te}_3$ . The formation energy of Cr- and V-doped  $(\text{Bi}, \text{Sb})_2\text{Te}_3$  as a function of chemical potential  $\mu_{\text{Te}}$  is studied to explore the most stable substitutional sites [see Figs. 3(b) and 3(c)]. One can observe that the formation energy of the Cr or V dopant in the Bi substitutional site is always lower than that in the Sb substitutional sites, indicating that Cr and V prefer Bi sites. In addition, the formation energy of the V dopant in the Bi site is much closer to those in  $\text{Sb}_{2,3}$  sites as displayed in Fig. 3(c), implying that the V dopant might also

TABLE I. Magnetic properties between two doped Cr or V magnetic elements at homogeneous and inhomogeneous  $(\text{Bi, Sb})_2\text{Te}_3$  systems. In our consideration,  $\text{Bi}_0$  and  $\text{Bi}_3$  are simultaneously substituted by magnetic dopants for the homogeneous case, whereas  $\text{Bi}_0$  and  $\text{Bi}_1$  sites for the inhomogeneous case.

Properties	Cr doping		V doping	
	Homo	Inhomo	Homo	Inhomo
$E_{\text{FM-AFM}}$ (meV)	-9.56	-54.37	-15.77	-73.33
Magnetic moment ( $\mu_B$ )	3.08	3.06	2.66	2.59
Curie temperature (K)	18.49	105.15	30.50	141.82

substitute in Sb sites except Bi sites in experiments. Thus, one can conclude that the Cr dopant prefers Bi sites, while the V dopant prefers both Bi and Sb sites, which might be related to the experimental finding that ferromagnetic homogeneity in Cr-doped  $(\text{Bi, Sb})_2\text{Te}_3$  can be enhanced by V codoping [37]. In the experiment of V- and Cr-codoped  $(\text{Bi, Sb})_2\text{Te}_3$ , Ou *et al.* also performed a transport study of the codoped  $(\text{Bi, Sb})_2\text{Te}_3$  with various Cr/V ratios and found that the optimized sample (Cr:V=16:84) has the most mean-field-like behavior, and V-doped samples are more mean-field-like than those of Cr dominantly doped ones, which agrees with the data from full width at half maximum (FWHM)/ $H_c$  and indicates that the samples with QAHE at higher temperatures also have reduced ferromagnetic inhomogeneity [37]. In Fig. S3, we also provide the relationship between the Cr/V ratio and mixing energy in codoped  $(\text{Bi, Sb})_2\text{Te}_3$ . For ease of comparison, the data of Cr or V single doping are also included. We can conclude that ferromagnetic homogeneity in V single doping and V and Cr codoping is better than that with Cr single doping, which is in qualitative agreement with the experimental finding. Based on our calculations, the ferromagnetic homogeneity in V single doping is identical to those in V- and Cr-codoped  $(\text{Bi, Sb})_2\text{Te}_3$  (Cr:V=2:1 or 1:3) at low codoping concentrations. It is also possible that the ferromagnetic homogeneity in codoped  $(\text{Bi, Sb})_2\text{Te}_3$  with a proper Cr/V ratio is superior to that of V single doping, as observed in an optimized sample (Cr:V=16:84) in experiments.

*Magnetic property and electronic structures of inhomogeneous  $(\text{Bi, Sb})_2\text{Te}_3$ .* Our above results show that the inhomogeneous mixing of Bi and Sb is the origin of the inhomogeneous phase in experimental  $(\text{Bi, Sb})_2\text{Te}_3$  systems. In the following, we will discuss the influence of the inhomogeneous distribution of Bi on the magnetic property of  $(\text{Bi, Sb})_2\text{Te}_3$ . First, we consider the magnetic couplings of inhomogeneous Cr and V doping in  $(\text{Bi, Sb})_2\text{Te}_3$  systems. For comparison, as listed in Table I, we calculate the magnetic coupling of homogeneous Cr- and V-doped  $(\text{Bi, Sb})_2\text{Te}_3$ . The magnetic coupling between the two doped magnetic elements at a given separation is evaluated by calculating the total energy difference between the ferromagnetic (FM) and the antiferromagnetic (AFM) configurations. From Table I, we can find that the magnetic couplings of inhomogeneous Cr and V doping in  $(\text{Bi, Sb})_2\text{Te}_3$  systems are FM coupling. Compared with those of homogeneous Cr and V doping in  $(\text{Bi, Sb})_2\text{Te}_3$  systems, magnetic couplings are stronger

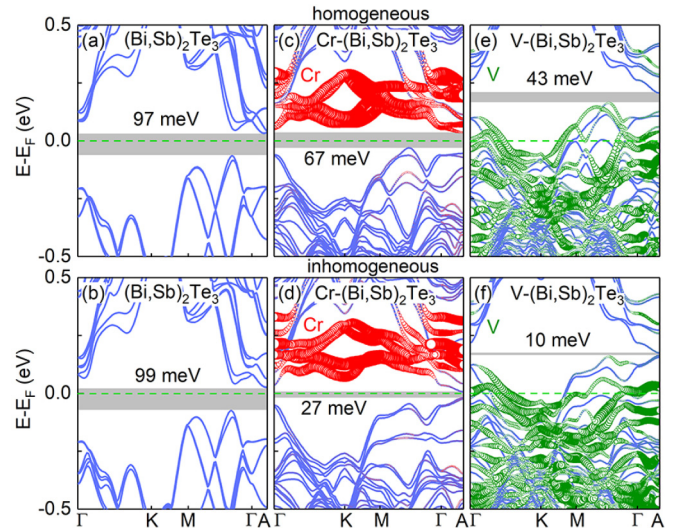


FIG. 4. (a), (b) Bulk band structures of (a) homogeneous and (b) inhomogeneous  $(\text{Bi, Sb})_2\text{Te}_3$  systems. (c), (d) Bulk band structures of (a) homogeneous and (b) inhomogeneous Bi and Sb mixing in Cr-doped  $(\text{Bi, Sb})_2\text{Te}_3$  systems. (e), (f) Bulk band structures of (e) homogeneous and (f) inhomogeneous Bi and Sb mixing in V-doped  $(\text{Bi, Sb})_2\text{Te}_3$  systems. The characters of the bands obtained by projecting the Kohn-Sham states onto the local orbitals of a single atom for the Cr/V element are also provided.

in inhomogeneous Cr- and V-doped  $(\text{Bi, Sb})_2\text{Te}_3$  systems. Thus, the estimated Curie temperatures of Cr- and V-doped inhomogeneous  $(\text{Bi, Sb})_2\text{Te}_3$  are also higher than those of homogeneous  $(\text{Bi, Sb})_2\text{Te}_3$  systems. The fundamental reasons are that doped magnetic elements in inhomogeneous systems have smaller distances than those in homogeneous systems. As shown in Fig. 1(b), in order to simulate the inhomogeneous and homogeneous doping of magnetic elements, two extreme cases were designed. One is that doped magnetic elements substitute the Bi atoms in the same atomic layer for the inhomogeneous case, and the other is that magnetic substitution happens in different quintuple layers (QLs) for the homogeneous  $(\text{Bi, Sb})_2\text{Te}_3$ . Hence, magnetic doping and related magnetic properties in experimental  $(\text{Bi, Sb})_2\text{Te}_3$  systems should be within the range of our simulated two extreme cases.

Next, we investigate the influence of inhomogeneous mixing of Bi and Sb on the band structures of Cr- and V-doped  $(\text{Bi, Sb})_2\text{Te}_3$  systems. As displayed in Figs. 4(a) and 4(b), the band structures, especially for band gaps, of homogeneous and inhomogeneous mixed  $(\text{Bi, Sb})_2\text{Te}_3$  show a negligible difference. After Cr and V doping, from Figs. 4(c)–4(f), we can find that the band gaps of homogeneous and inhomogeneous systems obviously decrease, originating from the Cr contribution to the conduction band minimum [Figs. 4(c) and 4(d)] or the V contribution to the valence band maximum [Figs. 4(e) and 4(f)]. In addition, we can also find that the bulk band gap of homogeneously mixed  $(\text{Bi, Sb})_2\text{Te}_3$  with Cr doping is about 67 meV, but it decreases to 27 meV in the inhomogeneously mixed case. Similarly, as displayed in Figs. 4(e) and 4(f), V-doping results give respectively 43 and 10 meV of bulk band gaps for the homogeneously and inhomogeneously mixed systems. As shown in Figs. 4 and S4, the gap decrease

of the inhomogeneous system in comparison to the homogeneous system is not directly related to the doped Cr or V element, but arises mainly from the Bi contribution to the valence band maximum [Figs. S4(a) and S4(g)]. All these findings show that the inhomogeneous mixing of Bi and Sb results in obvious decreases of the bulk band gaps of  $(\text{Bi, Sb})_2\text{Te}_3$  systems, whereas the homogeneous mixing of Bi and Sb is beneficial to the formation of high-temperature QAHE.

Based on the above findings, it strongly suggests that the homogeneous mixing of Bi and Sb in  $(\text{Bi, Sb})_2\text{Te}_3$  systems is crucial in realizing high-temperature QAHE. An effective way to experimentally reduce the magnetic inhomogeneity in  $(\text{Bi, Sb})_2\text{Te}_3$  is to reduce the inhomogeneous mixing of Bi and Sb elements during the process of material fabrication. If the obstacle can be solved, a higher QAHE observation temperature will be expected. Our analysis also indicates that V doping in a homogeneously mixed  $(\text{Bi, Sb})_2\text{Te}_3$  system will be a good candidate for high-temperature QAHE.

*Summary.* Our systematic studies demonstrate that the intrinsic origin of inhomogeneous ferromagnetism is the inhomogeneous mixing of Bi and Sb in  $(\text{Bi, Sb})_2\text{Te}_3$ , but not the doped magnetic-impurity-induced disorder. Moreover, the formation energies of Cr and V show that they prefer to substitute Bi sites in inhomogeneously mixed  $(\text{Bi, Sb})_2\text{Te}_3$  systems. Our findings will shed light on the experimental enhancement of the QAHE observation temperature in magnetically doped topological insulators.

*Acknowledgments.* This work was financially supported by the National Key R&D Program (2017YFB0405703), NNSFC (11974098 and 11974327), Natural Science Foundation of Hebei Province (A2019205037), Science Foundation of Hebei Normal University (2019B08), Anhui Initiative in Quantum Information Technologies, and the Fundamental Research Funds for the Central Universities. We are grateful to AMHPC and Supercomputing Center of USTC for providing the high-performance computing resources.

- 
- [1] F. D. M. Haldane, *Phys. Rev. Lett.* **61**, 2015 (1988).  
 [2] K. He, Y. Wang, and Q.-K. Xue, *Annu. Rev. Condens. Matter Phys.* **9**, 329 (2018).  
 [3] Y. Ren, Z. Qiao, and Q. Niu, *Rep. Prog. Phys.* **79**, 066501 (2016).  
 [4] N. Nagaosa, J. Sinova, S. Onoda, A. H. MacDonald, and N. P. Ong, *Rev. Mod. Phys.* **82**, 1539 (2010).  
 [5] K. von Klitzing, *Rev. Mod. Phys.* **58**, 519 (1986).  
 [6] K. S. Novoselov, A. K. Geim, S. V. Morozov, D. Jiang, Y. Zhang, S. V. Dubonos, I. V. Grigorieva, and A. A. Firsov, *Science* **306**, 666 (2004).  
 [7] M. Onoda and N. Nagaosa, *Phys. Rev. Lett.* **90**, 206601 (2003).  
 [8] C. X. Liu, X. L. Qi, X. Dai, Z. Fang, and S. C. Zhang, *Phys. Rev. Lett.* **101**, 146802 (2008).  
 [9] C. Wu, *Phys. Rev. Lett.* **101**, 186807 (2008).  
 [10] R. Yu, W. Zhang, H. J. Zhang, S. C. Zhang, X. Dai, and Z. Fang, *Science* **329**, 61 (2010).  
 [11] Z. H. Qiao, S. A. Yang, W. X. Feng, W.-K. Tse, J. Ding, Y. G. Yao, J. Wang, and Q. Niu, *Phys. Rev. B* **82**, 161414(R) (2010).  
 [12] Z. F. Wang, Z. Liu, and F. Liu, *Phys. Rev. Lett.* **110**, 196801 (2013).  
 [13] K. F. Garrity and D. Vanderbilt, *Phys. Rev. Lett.* **110**, 116802 (2013).  
 [14] J. Hu, Z. Zhu, and R. Wu, *Nano Lett.* **15**, 2074 (2015).  
 [15] C. Fang, M. J. Gilbert, and B. A. Bernevig, *Phys. Rev. Lett.* **112**, 046801 (2014).  
 [16] J. Wang, B. Lian, H. Zhang, Y. Xu, and S. C. Zhang, *Phys. Rev. Lett.* **111**, 136801 (2013).  
 [17] G. F. Zhang, Y. Li, and C. Wu, *Phys. Rev. B* **90**, 075114 (2014).  
 [18] H. Z. Lu, A. Zhao, and S. Q. Shen, *Phys. Rev. Lett.* **111**, 146802 (2013).  
 [19] M. Z. Hasan and C. L. Kane, *Rev. Mod. Phys.* **82**, 3045 (2010).  
 [20] X. L. Qi and S. C. Zhang, *Rev. Mod. Phys.* **83**, 1057 (2011).  
 [21] K. He and Q.-K. Xue, *Nat. Sci. Rev.* **6**, 202 (2019).  
 [22] S. Qi, R. Gao, M. Chang, Y. Han, and Z. Qiao, *Phys. Rev. B* **101**, 014423 (2020).  
 [23] Y. S. Hor, P. Roushan, H. Beidenkopf, J. Seo, D. Qu, J. G. Checkelsky, L. A. Wray, D. Hsieh, Y. Xia, S. Y. Xu, D. Qian, M. Z. Hasan, N. P. Ong, A. Yazdani, and R. J. Cava, *Phys. Rev. B* **81**, 195203 (2010).  
 [24] C. Niu, Y. Dai, M. Guo, W. Wei, Y. Ma, and B. Huang, *Appl. Phys. Lett.* **98**, 252502 (2011).  
 [25] P. P. J. Haazen, J. B. Laloe, T. J. Nummy, H. J. M. Swagten, P. Jarillo-Herrero, D. Heiman, and J. S. Moodera, *Appl. Phys. Lett.* **100**, 082404 (2012).  
 [26] T. Jungwirth, J. Sinova, J. Masek, J. Kucera, and A. H. MacDonald, *Rev. Mod. Phys.* **78**, 809 (2006).  
 [27] C.-Z. Chang, J. S. Zhang, X. Feng, J. Shen, Z. C. Zhang, M. Guo, K. Li, Y. Ou, P. Wei, L.-L. Wang, Z.-Q. Ji, Y. Feng, S. H. Ji, X. Chen, J. F. Jia, X. Dai, Z. Fang, S.-C. Zhang, K. He, Y. Y. Wang *et al.*, *Science* **340**, 167 (2013).  
 [28] J. G. Checkelsky, R. Yoshimi, A. Tsukazaki, K. S. Takahashi, Y. Kozuka, J. Falson, M. Kawasaki, and Y. Tokura, *Nat. Phys.* **10**, 731 (2014).  
 [29] X. Kou, S.-T. Guo, Y. Fan, L. Pan, M. Lang, Y. Jiang, Q. Shao, T. Nie, K. Murata, J. Tang, Y. Wang, L. He, T.-K. Lee, W.-L. Lee, and K. L. Wang, *Phys. Rev. Lett.* **113**, 137201 (2014).  
 [30] C. Z. Chang, W. Zhao, D. Y. Kim, H. Zhang, B. A. Assaf, D. Heiman, S.-C. Zhang, C. Liu, M. H. W. Chan, and J. S. Moodera, *Nat. Mater.* **14**, 473 (2015).  
 [31] S. Grauer, S. Schreyeck, M. Winnerlein, K. Brunner, C. Gould, and L. W. Molenkamp, *Phys. Rev. B* **92**, 201304(R) (2015).  
 [32] I. Lee, C. K. Kima, J. Leea, S. J. L. Billingea, R. Zhong, J. A. Schneeloch, T. Liua, T. Valla, J. M. Tranquada, G. Gua, and J. C. S. Davis, *Proc. Natl. Acad. Sci. USA* **112**, 1316 (2015).  
 [33] E. O. Lachman, A. F. Young, A. Richardella, J. Cuppens, H. R. Naren, Y. Anahory, A. Y. Meltzer, A. Kandala, S. Kempinger, Y. Myasoedov, M. E. Huber, N. Samarth, and E. Zeldov, *Sci. Adv.* **1**, e1500740 (2015).  
 [34] X. Feng, Y. Feng, J. Wang, Y. Ou, Z. Hao, C. Liu, Z. Zhang, L. Zhang, C. Lin, J. Liao, Y. Li, L.-L. Wang, S.-H. Ji, X. Chen, X. Ma, S.-C. Zhang, Y. Wang, K. He, and Q.-K. Xue, *Adv. Mater.* **28**, 6386 (2016).  
 [35] M. Mogi, R. Yoshimi, A. Tsukazaki, K. Yasuda, Y. Kozuka, K. S. Takahashi, and Y. Tokura, *Appl. Phys. Lett.* **107**, 182401 (2015).

- [36] S. Qi, Z. Qiao, X. Deng, E. D. Cubuk, H. Chen, W. Zhu, E. Kaxiras, S. B. Zhang, X. Xu, and Z. B. Zhang, *Phys. Rev. Lett.* **117**, 056804 (2016).
- [37] Y. Ou, C. Liu, G. Y. Jiang, Y. Feng, D. Y. Zhao, W. X. Wu, X. X. Wang, W. Li, C. L. Song, L. L. Wang, W. B. Wang, W. D. Wu, Y. Y. Wang, K. He, X. C. Ma, and Q. K. Xue, *Adv. Mater.* **30**, 1703062 (2018).
- [38] S. Qi, F. Jiang, J. Fan, H. Wu, S. B. Zhang, G. A. Gehring, Z. Zhang, and X. Xu, *Phys. Rev. B* **84**, 205204 (2011).
- [39] T. Dietl and H. Ohno, *Rev. Mod. Phys.* **86**, 187 (2014).
- [40] P. E. Blöchl, *Phys. Rev. B* **50**, 17953 (1994).
- [41] G. Kresse and J. Furthmüller, *Phys. Rev. B* **54**, 11169 (1996).
- [42] J. P. Perdew, J. A. Chevary, S. H. Vosko, K. A. Jackson, M. R. Pederson, D. J. Singh, and C. Fiolhais, *Phys. Rev. B* **46**, 6671 (1992).
- [43] V. I. Anisimov, J. Zaanen, and O. K. Andersen, *Phys. Rev. B* **44**, 943 (1991).
- [44] L. Bergqvist, P. A. Korzhavyi, B. Sanyal, S. Mirbt, I. A. Abrikosov, L. Nordström, E. A. Smirnova, P. Mohn, P. Svedlindh, and O. Eriksson, *Phys. Rev. B* **67**, 205201 (2003).
- [45] K. Sato, L. Bergqvist, J. Kudrnovsky, P. H. Dederichs, O. Eriksson, I. Turek, B. Sanyal, G. Bouzerar, H. Katayama-Yoshida, V. A. Dinh, T. Fukushima, H. Kizaki, and R. Zeller, *Rev. Mod. Phys.* **82**, 1633 (2010).
- [46] See Supplemental Material at <http://link.aps.org/supplemental/10.1103/PhysRevB.101.241407> for the test calculation on Mn-doped GaAs, mixing energies of Cr- and V-codoped TIs with different defects, relationship between Cr/V ratio and mixing energy, and different characters of the bands for Cr- and V-codoped homogeneous and inhomogeneous (Bi, Sb)<sub>2</sub>Te<sub>3</sub> systems, which includes Ref. [44].
- [47] J. M. Zhang, W. G. Zhu, Y. Zhang, D. Xiao, and Y. G. Yao, *Phys. Rev. Lett.* **109**, 266405 (2012).
- [48] K. Sato and H. Katayama-Yoshida, *Jpn. J. Appl. Phys.* **46**, L1120 (2007).
- [49] A. Bonanni, *Semicond. Sci. Technol.* **22**, R41 (2007).
- [50] R. N. Zitter and P. T. Watson, *Phys. Rev. B* **10**, 607 (1974).
- [51] H. Plank, S. N. Danilov, V. V. Belkov, V. A. Shalygin, J. Kampmeier, M. Lanius, G. Mussler, D. Grutzmacher, and S. D. Ganichev, *J. Appl. Phys.* **120**, 165301 (2016).